Palestine Journal of Mathematics

Vol. 11(Special Issue I)(2022) , 184–201

AN ANALYTICAL STUDY OF NON-NEWTONIAN VISCO-INELASTIC FLUID FLOW BETWEEN TWO STRETCHABLE ROTATING DISKS

Reshu Agarwal

Communicated by Muslim Malik

MSC 2010 Classifications: Primary 20M99, 13F10; Secondary 13A15, 13M05.

Keywords and phrases: Reiner-Rivlin Fluid, Rotating Disks, Homotopy Perturbation Method, Numerical Method, Stretchable Disks.

Abstract In this article, non-Newtonian visco-inelastic fluid flow between two disks is investigated analytically. In this model, both disks are rotating about a $z-$axis and stretching radially. The obtained higher-order, partial differential equations (PDEs) are reconstructed into a system of nonlinear ordinary differential equations (ODEs) by using similarity transformation. Homotopy Perturbation Method (HPM) is used to get the solution of obtained coupled ODEs bounded with conditions. This model is discussed under the following cases when (1) the upper disk is getting stretched but the lower disk is not stretched (2) both disks are getting stretched (3) the lower disk is getting stretched but the upper disk is not stretched. The impact of different physical parameters on radial, transverse and axial velocities are presented graphically in all three cases. The results of Newtonian fluid have also been shown by putting non-Newtonian parameter zero. The accuracy of the results evaluated by HPM is confirmed by numerical results. A comparison of shear stress on the lower disk in the radial and tangential direction of the present study is shown with the literature's value.

1 Introduction

In the last decades, the discussed model has been a huge interest area of researchers. Consequently, several Mathematicians have studied the same model under various physical and experimental conditions. Batchelor [5] has generated Von-Karman's solution [30] of the Navier-Stokes equations describing the steady viscous flow near a rotating disk. The flow between two rotating coaxial disks has been discussed by Stewartson [24]. Cochran [6] discussed the flow due to a rotating disk. The axially symmetric flow of a viscous fluid between two infinite rotating disks has been investigated by Lance and Rogers [16]. Heat transfer in the forced flow of visco-inelastic fluid between two infinite disks was studied by Singh and Agarwal [23]. Mustafa [28] and Das [9] discussed flow in two stretchable rotating disks. Numerical treatment for parallel slip flow was investigated by Tabassum and Mustafa [25] and its numerical study has been done by Naqui [18]. Sahoo [21]-[22] discussed heat transfer and revolving flow in Reiner-Rivlin fluid. The same model for coaxial rotating disk was discussed by Das [8]. Zangooeel et al. [34], Yao and lian [33] and Yao and Lian [32] studied the disk model for different fluids by analytical method. Usman et al. [29] have been studied heat transfer from a non-isothermal rotating rough disk subjected to forced flow. Hayat et al. [12] studied the convective flow of Jeffrey nanofluid due to two stretchable rotating disks. Numerical analysis of the sound radiation from rotating in the presence of transverse magnet disks has been discussed by Maeder et al. [17].Turkyilmazoglu [26] and [27] discussed the model of a rotating disk. Agarwal [1],[3] and [2] discussed some models in her studies.

The HPM is a well-known method to find out nonlinear partial and ordinary differential equations. This method has been proven very commanding in a variety of problems in different fields. In many fluid mechanics problems, equations of flow and heat transfer are nonlinear, to get their solutions many researchers use a numerical approach and some of them applied analytical methods such as perturbation technique.

The HPM is firstly introduced by He [13] in 1999 who [15]-[14] also did some modification. The HPM has been shown to solve a large class of nonlinear problems efficiently, accurately, and easily. The HPM has been applied in the disk model by Donald [4]. Homogenous and heterogeneous reactions in a nanofluid flow due to a rotating disk of variable thickness using HAM were studied by Doh et al. [11]. Dinarvand [10] has discussed an explicit, purely analytic solution of off-centered stagnation flow towards a rotating disk using HAM. An analytic approximate solution for study flow over a rotating disk in a porous medium with heat transfer by HAM has been investigated by Rashidi et al. [20]. Jansi et al. [19] have employed HPM to achieve the solution of their problem. Xinhui et al. [31] have discussed flow and heat transfer of viscous fluid between contracting rotating disks by HAM.

The main target of this article is to analyze the flow characteristics of Reiner-Rivlin fluid, which is confined between two rotating stretchable disks by using HPM. The observation of radial, transverse, and axial velocity components have been presented graphically for several values of Reynolds number R_o, the non-Newtonian parameter N, and rotation parameter A. To check the validity of HPM, obtained results are matched with numerical method results. A comparison of shear stress on the lower disk in the radial and tangential direction of the present study is shown with the literature's value. Also putting the value of non-Newtonian parameter $N = 0$, the fluid follows Newtonian behavior.

2 Mathematical Model

The consecutive equation for Reiner-Rivlin fluid as mentioned by Coleman and Noll [7] is as follows

$$\tau_{ij} = -p\delta_{ij} + 2\mu_{nv}d_{ij} + 4\mu_{cv}c_{ij} \tag{2.1}$$

where

$$\begin{aligned} d_{ij} &= \frac{1}{2}\left(u_{i,j} + u_{j,i}\right) \\ c_{ij} &= d_{im}d^m_j \end{aligned} \tag{2.2}$$

$\tau_{ij}, p, \delta_{ij}, \rho, \mu_{nv}$ and μ_{cv} are stress-tensor, hydrostatic pressure, Kronecker's delta tensor, density, coefficient of Newtonian-viscosity and coefficient of cross-viscosity respectively. d_{ij}, c_{ij} are the symmetric tensors and u_i is velocity vector. The author used cylindrical coordinates (r, θ, z)

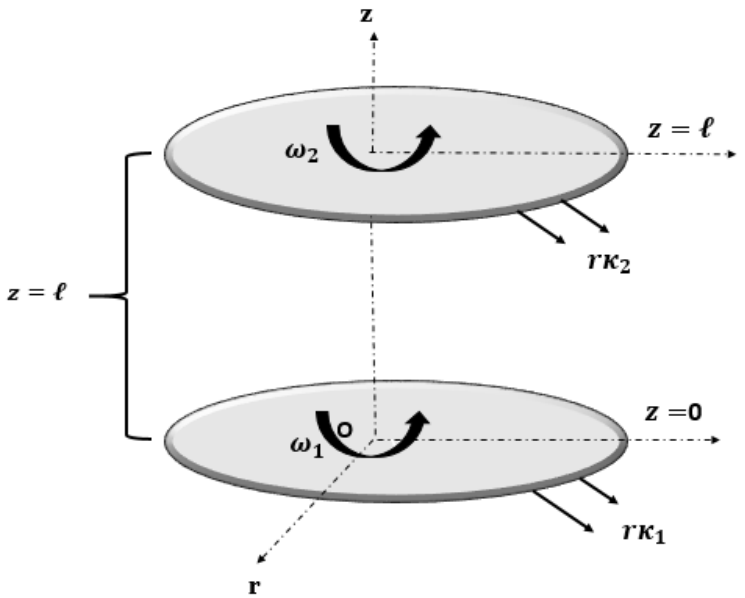

Figure 1: Flow model of the stretchable disks

here. The non-Newtonian fluid is filled between two rotating disks at a distance ℓ apart. The disk

coinciding with the plane $z = 0$ rotates along the $z-$axis with angular velocity ω_1 and stretches radially with the constant rate κ_1. The disk situated at the plane $z = \ell$ rotates along the $z-$axis with angular velocity ω_2 and stretches radially with the constant rate κ_2. Let u, v and w are the velocities in r, θ and z direction respectively, and $\frac{\partial}{\partial\theta} = 0$ (due to symmetrical rotation)
The equation of continuity and momentum equations are

$$\frac{\partial u}{\partial r} + \frac{u}{r} + \frac{\partial w}{\partial z} = 0 \tag{2.3}$$

$$\rho\left(u\frac{\partial u}{\partial r} - \frac{v^2}{r} + w\frac{\partial u}{\partial z}\right) = \frac{\partial \tau_{rr}}{\partial r} + \frac{\partial \tau_{rz}}{\partial z} + \frac{\tau_{rr} - \tau_{\theta\theta}}{r} \tag{2.4}$$

$$\rho\left(u\frac{\partial v}{\partial r} + \frac{uv}{r} + w\frac{\partial v}{\partial z}\right) = \frac{\partial \tau_{r\theta}}{\partial r} + \frac{\partial \tau_{\theta z}}{\partial z} + \frac{2\tau_{r\theta}}{r} \tag{2.5}$$

$$\rho\left(u\frac{\partial w}{\partial r} + w\frac{\partial w}{\partial z}\right) = \frac{\partial \tau_{zr}}{\partial r} + \frac{\partial \tau_{zz}}{\partial z} + \frac{\tau_{rz}}{r} \tag{2.6}$$

The boundary conditions of the present model are

$$\begin{aligned} z = 0: &\quad u = r\kappa_1, \quad v = r\omega_1, \quad w = 0, \\ z = \ell: &\quad u = r\kappa_2, \quad v = r\omega_2, \quad w = 0. \end{aligned} \tag{2.7}$$

The velocity profile as suggested by Von Karman [30] is given by

$$\begin{aligned} u &= r\omega_1 f^{'}(\xi) \\ v &= r\omega_1 h(\xi) \\ w &= -2\ell\omega_1 f(\xi) \end{aligned} \tag{2.8}$$

where $\xi = \frac{z}{\ell}$ is a dimensionless parameter.
The obtained higher-order, PDEs are now reformed into a system of nonlinear ODEs. So by using Equation (2.8) in Equation (2.4)-(2.6), we get

$$f^{iv} + 2R_o\left(hh^{'} + ff^{'''}\right) - NR_o\left(f^{'}f^{iv} + 3h^{'}h^{''} + 2f^{''}f^{'''}\right) = 0 \tag{2.9}$$

$$h^{''} + 2R_o\left(fh^{'} - f^{'}h\right) + NR_o\left(f^{''}h^{'} - f^{'}h^{''}\right) = 0 \tag{2.10}$$

Reduced boundary conditions are

$$\begin{aligned} \xi = 0: &\quad f = 0, \quad h = 1, \quad f^{'} = K_1, \\ \xi = 1: &\quad f = 0, \quad h = A, \quad f^{'} = K_2. \end{aligned} \tag{2.11}$$

where $R_o = \frac{\omega_1\ell^2}{\mu_{nv}}$, is the Reynolds number, $K_1 = \frac{\kappa_1}{\omega_1}$ and $K_2 = \frac{\kappa_2}{\omega_2}$ are stretching parameters, A=$\frac{\omega_2}{\omega_1}$ is a rotation number and $N = \frac{2\mu_{cv}}{\rho\ell^2}$ in non-Newtonian parameter.

3 Methodology

3.1 Description of Method

According to He [13], to describe the fundamentals of HPM, we form the equation

$$K(u) - m(r) = 0, \qquad r\epsilon\Omega \tag{3.1}$$

with the boundary conditions

$$\beta\left(u, \frac{\partial u}{\partial n}\right) = 0, \qquad r\epsilon\delta \tag{3.2}$$

Distribute $K(u)$ in $L_r(u)$ and $N_r(u)$ where $L_r(u)$ is linear, $N_r(u)$ is nonlinear and $m(r)$ is known analytic function.
$\therefore$ We can rewrite Equation (3.1) as

$$L_r(u) + N_r(u) - m(r) = 0, \qquad r\epsilon\Omega \tag{3.3}$$

The homotopy can be defined as

$$H(u,\epsilon) = (1-\epsilon))\left[L_r(u) - L_r(u_0)\right] + \epsilon\left[K(u) - m(r)\right] = 0 \tag{3.4}$$

where

$$u(r,\epsilon) : \Omega \times [0,1] \to R \tag{3.5}$$

In equation (3.5), ϵ is an embedded parameter which lies between $[0,1]$ and u_0 is the initial approximation which satisfies the boundary condition.
The solution of equation (3.4) in the power of ϵ can be written as

$$u = u_0 + \epsilon u_1 + \epsilon^2 u_2 + ----- \tag{3.6}$$

Hence the best result is

$$u = \lim_{\epsilon\to 1} u = u_0 + u_1 + u_2 + ---- \tag{3.7}$$

3.2 Implementation of the Method

A homotopy for equations (2.9) and (2.10) are

$$H(f,\epsilon) = (1-\epsilon))\left[f^{iv} - f_0^{iv}\right] + \epsilon\left[f^{iv} + 2R_o\left(hh^{'} + ff^{'''}\right) - NR_o\left(f^{'}f^{iv} + 3h^{'}h^{''} + 2f^{''}f^{'''}\right)\right] = 0 \tag{3.8}$$

$$H(h,\epsilon) = (1-\epsilon))\left[h^{''} - h_0^{''}\right] + \epsilon\left[h^{''} + 2R_o\left(fh^{'} - f^{'}h\right) + NR_o\left(f^{''}h^{'} - f^{'}h^{''}\right)\right] = 0 \tag{3.9}$$

where ϵ lies between 0 and 1. f_0 and h_0 are an initial approximation that satisfies conditions at the boundary. Consider approximate outcomes of equations (3.8) and (3.9) in the ascending power of ϵ are

$$f(\xi) = \sum_{i=0}^{\infty} f_i\epsilon^i = f_0(\xi) + \epsilon f_1(\xi) + \epsilon^2 f_2(\xi) + ------ \tag{3.10}$$

$$h(\xi) = \sum_{i=0}^{\infty} h_i\epsilon^i = h_0(\xi) + \epsilon h_1(\xi) + \epsilon^2 h_2(\xi) + ------ \tag{3.11}$$

For the best approximation for solution at $\epsilon \to 1$ is

$$f = f_0 + f_1 + f_2 + f_3 + ---- \tag{3.12}$$

$$h = h_0 + h_1 + h_2 + h_3 + ---- \tag{3.13}$$

coefficient of ϵ^0:

$$\frac{\mathrm{d}^4}{\mathrm{d}\xi^4} f_0(\xi) = 0 \tag{3.14}$$

$$\frac{\mathrm{d}^2}{\mathrm{d}\xi^2}h_0(\xi)=0 \tag{3.15}$$

coefficient of ϵ^1:

$$\frac{\mathrm{d}^4}{\mathrm{d}\xi^4}f_1(\xi)+2R_o\left(h_0(\xi)\frac{\mathrm{d}}{\mathrm{d}\xi}h_0(\xi)+f_0(\xi)\frac{\mathrm{d}^3}{\mathrm{d}\xi^3}f_0(\xi)\right)$$
$$-NR_o\Bigg(\left(\frac{\mathrm{d}}{\mathrm{d}\xi}f_0(\xi)\right)\frac{\mathrm{d}^4}{\mathrm{d}\xi^4}f_0(\xi)+3\left(\frac{\mathrm{d}}{\mathrm{d}\xi}h_0(\xi)\right)\frac{\mathrm{d}^2}{\mathrm{d}\xi^2}h_0(\xi)$$
$$+2\left(\frac{\mathrm{d}^2}{\mathrm{d}\xi^2}f_0(\xi)\right)\frac{\mathrm{d}^3}{\mathrm{d}\xi^3}f_0(\xi)\Bigg)=0 \tag{3.16}$$

$$\frac{\mathrm{d}^2}{\mathrm{d}\xi^2}h_1(\xi)+2R_o\left(f_0(\xi)\frac{\mathrm{d}}{\mathrm{d}\xi}h_0(\xi)-\left(\frac{\mathrm{d}}{\mathrm{d}\xi}f_0(\xi)\right)h_0(\xi)\right)$$
$$+NR_o\Bigg(\left(\frac{\mathrm{d}^2}{\mathrm{d}\xi^2}f_0(\xi)\right)\frac{\mathrm{d}}{\mathrm{d}\xi}h_0(\xi)-\left(\frac{\mathrm{d}}{\mathrm{d}\xi}f_0(\xi)\right)\frac{\mathrm{d}^2}{\mathrm{d}\xi^2}h_0(\xi)\Bigg)=0 \tag{3.17}$$

coefficient of ϵ^2:

$$\frac{\mathrm{d}^4}{\mathrm{d}\xi^4}f_2(\xi)+2R_o\Bigg(h_0(\xi)\frac{\mathrm{d}}{\mathrm{d}\xi}h_1(\xi)+h_1(\xi)\frac{\mathrm{d}}{\mathrm{d}\xi}h_0(\xi)+f_0(\xi)\frac{\mathrm{d}^3}{\mathrm{d}\xi^3}f_1(\xi)$$
$$+f_1(\xi)\frac{\mathrm{d}^3}{\mathrm{d}\xi^3}f_0(\xi)\Bigg)-NR_o\Bigg(\left(\frac{\mathrm{d}}{\mathrm{d}\xi}f_0(\xi)\right)\frac{\mathrm{d}^4}{\mathrm{d}\xi^4}f_1(\xi)$$
$$+\left(\frac{\mathrm{d}}{\mathrm{d}\xi}f_1(\xi)\right)\frac{\mathrm{d}^4}{\mathrm{d}\xi^4}f_0(\xi)+3\left(\frac{\mathrm{d}}{\mathrm{d}\xi}h_0(\xi)\right)\frac{\mathrm{d}^2}{\mathrm{d}\xi^2}h_1(\xi)+3\left(\frac{\mathrm{d}}{\mathrm{d}\xi}h_1(\xi)\right)\frac{\mathrm{d}^2}{\mathrm{d}\xi^2}h_0(\xi)$$
$$+2\left(\frac{\mathrm{d}^2}{\mathrm{d}\xi^2}f_0(\xi)\right)\frac{\mathrm{d}^3}{\mathrm{d}\xi^3}f_1(\xi)+2\left(\frac{\mathrm{d}^2}{\mathrm{d}\xi^2}f_1(\xi)\right)\frac{\mathrm{d}^3}{\mathrm{d}\xi^3}f_0(\xi)\Bigg)=0 \tag{3.18}$$

$$\frac{\mathrm{d}^2}{\mathrm{d}\xi^2}h_2(\xi)+2R_o\Bigg(f_0(\xi)\frac{\mathrm{d}}{\mathrm{d}\xi}h_1(\xi)+f_1(\xi)\frac{\mathrm{d}}{\mathrm{d}\xi}h_0(\xi)-\left(\frac{\mathrm{d}}{\mathrm{d}\xi}f_0(\xi)\right)h_1(\xi)$$
$$-\left(\frac{\mathrm{d}}{\mathrm{d}\xi}f_1(\xi)\right)h_0(\xi)\Bigg)+NR_o\Bigg(\left(\frac{\mathrm{d}^2}{\mathrm{d}\xi^2}f_0(\xi)\right)\frac{\mathrm{d}}{\mathrm{d}\xi}h_1(\xi)$$
$$+\left(\frac{\mathrm{d}^2}{\mathrm{d}\xi^2}f_1(\xi)\right)\frac{\mathrm{d}}{\mathrm{d}\xi}h_0(\xi)\Bigg)-NR_o\Bigg(\left(\frac{\mathrm{d}}{\mathrm{d}\xi}f_0(\xi)\right)\frac{\mathrm{d}^2}{\mathrm{d}\xi^2}h_1(\xi)$$
$$+\left(\frac{\mathrm{d}}{\mathrm{d}\xi}f_1(\xi)\right)\frac{\mathrm{d}^2}{\mathrm{d}\xi^2}h_0(\xi)\Bigg)=0 \tag{3.19}$$

coefficient of ϵ^3:

$$\frac{\mathrm{d}^4}{\mathrm{d}\xi^4} f_3(\xi) + 2R_o\Bigg(h_0(\xi)\frac{\mathrm{d}}{\mathrm{d}\xi} h_2(\xi) + h_1(\xi)\frac{\mathrm{d}}{\mathrm{d}\xi} h_1(\xi) + h_2(\xi)\frac{\mathrm{d}}{\mathrm{d}\xi} h_0(\xi) + f_0(\xi)\frac{\mathrm{d}^3}{\mathrm{d}\xi^3} f_2(\xi) + f_1(\xi)\frac{\mathrm{d}^3}{\mathrm{d}\xi^3} f_1(\xi)\Bigg) + 2R_o\Bigg(f_2(\xi)\frac{\mathrm{d}^3}{\mathrm{d}\xi^3} f_0(\xi)\Bigg) - NR_o\Bigg(\Bigg(\frac{\mathrm{d}}{\mathrm{d}\xi} f_0(\xi)\Bigg)\frac{\mathrm{d}^4}{\mathrm{d}\xi^4} f_2(\xi) + \Bigg(\frac{\mathrm{d}}{\mathrm{d}\xi} f_1(\xi)\Bigg)\frac{\mathrm{d}^4}{\mathrm{d}\xi^4} f_1(\xi) + \Bigg(\frac{\mathrm{d}}{\mathrm{d}\xi} f_2(\xi)\Bigg)\frac{\mathrm{d}^4}{\mathrm{d}\xi^4} f_0(\xi)\Bigg) - 3NR_o\Bigg(\Bigg(\frac{\mathrm{d}}{\mathrm{d}\xi} h_0(\xi)\Bigg)\frac{\mathrm{d}^2}{\mathrm{d}\xi^2} h_2(\xi) + \Bigg(\frac{\mathrm{d}}{\mathrm{d}\xi} h_1(\xi)\Bigg)\frac{\mathrm{d}^2}{\mathrm{d}\xi^2} h_1(\xi) + \Bigg(\frac{\mathrm{d}}{\mathrm{d}\xi} h_2(\xi)\Bigg)\frac{\mathrm{d}^2}{\mathrm{d}\xi^2} h_0(\xi)\Bigg) - 2NR_o\Bigg(\Bigg(\frac{\mathrm{d}^2}{\mathrm{d}\xi^2} f_0(\xi)\Bigg)\frac{\mathrm{d}^3}{\mathrm{d}\xi^3} f_2(\xi) + \Bigg(\frac{\mathrm{d}^2}{\mathrm{d}\xi^2} f_1(\xi)\Bigg)\frac{\mathrm{d}^3}{\mathrm{d}\xi^3} f_1(\xi) + \Bigg(\frac{\mathrm{d}^2}{\mathrm{d}\xi^2} f_2(\xi)\Bigg)\frac{\mathrm{d}^3}{\mathrm{d}\xi^3} f_0(\xi)\Bigg) = 0 \quad (3.20)$$

$$\frac{\mathrm{d}^2}{\mathrm{d}\xi^2} h_3(\xi) + 2R_o\Bigg(f_0(\xi)\frac{\mathrm{d}}{\mathrm{d}\xi} h_2(\xi) + f_1(\xi)\frac{\mathrm{d}}{\mathrm{d}\xi} h_1(\xi) + f_2(\xi)\frac{\mathrm{d}}{\mathrm{d}\xi} h_0(\xi) - \Bigg(\frac{\mathrm{d}}{\mathrm{d}\xi} f_0(\xi)\Bigg) h_2(\xi)\Bigg) - 2R_o\Bigg(\Bigg(\frac{\mathrm{d}}{\mathrm{d}\xi} f_1(\xi)\Bigg) h_1(\xi) + \Bigg(\frac{\mathrm{d}}{\mathrm{d}\xi} f_2(\xi)\Bigg) h_0(\xi)\Bigg) + NR_o\Bigg(\Bigg(\frac{\mathrm{d}^2}{\mathrm{d}\xi^2} f_0(\xi)\Bigg)\frac{\mathrm{d}}{\mathrm{d}\xi} h_2(\xi)\Bigg) + NR_o\Bigg(\Bigg(\frac{\mathrm{d}^2}{\mathrm{d}\xi^2} f_1(\xi)\Bigg)\frac{\mathrm{d}}{\mathrm{d}\xi} h_1(\xi) + \Bigg(\frac{\mathrm{d}^2}{\mathrm{d}\xi^2} f_2(\xi)\Bigg)\frac{\mathrm{d}}{\mathrm{d}\xi} h_0(\xi) - \Bigg(\frac{\mathrm{d}}{\mathrm{d}\xi} f_0(\xi)\Bigg)\frac{\mathrm{d}^2}{\mathrm{d}\xi^2} h_2(\xi)\Bigg) - NR_o\Bigg(\Bigg(\frac{\mathrm{d}}{\mathrm{d}\xi} f_1(\xi)\Bigg)\frac{\mathrm{d}^2}{\mathrm{d}\xi^2} h_1(\xi) + \Bigg(\frac{\mathrm{d}}{\mathrm{d}\xi} f_2(\xi)\Bigg)\frac{\mathrm{d}^2}{\mathrm{d}\xi^2} h_0(\xi)\Bigg) = 0 \quad (3.21)$$

Solving equations (3.14)-(3.21) with boundary conditions given below

$$\begin{aligned} &f_n(0) = 0\ \forall n \geq 0, \quad f_0'(0) = K_1, \quad f_n'(0) = 0\ \forall n \geq 1, \quad h_0(0) = 1, \quad h_n(0) = 0\ \forall n \geq 1 \\ &f_n(1) = 0\ \forall n \geq 0, \quad f_0'(1) = K_2, \quad f_n'(1) = 0\ \forall n \geq 1, \quad h_0(1) = A, \quad h_n(1) = 0\ \forall n \geq 1 \end{aligned} \quad (3.22)$$

After simplification, we get

$$f_0(\xi) = 1/6\ (6K_2 + 6K_1)\xi^3 + 1/2\ (-2K_2 - 4K_1)\xi^2 + K_1\xi \quad (3.23)$$

$$h_0(\xi) = (A-1)\xi + 1 \quad (3.24)$$

$$
\begin{aligned}
f_1(\xi) &= -2R_o\left(\frac{\xi^7 {K_1}^2}{140}+\frac{\xi^7 K_1K_2}{70}+\frac{\xi^7 {K_2}^2}{140}-3/10\,N\xi^5 {K_1}^2-3/5\,N\xi^5K_1K_2\right.\\
&- 3/10\,N\xi^5{K_2}^2-1/30\,\xi^6{K_1}^2-1/20\,\xi^6K_1K_2-\frac{\xi^6{K_2}^2}{60}+\frac{A^2\xi^5}{120}+N\xi^4{K_1}^2\\
&+ 3/2\,N\xi^4K_1K_2+1/2\,N\xi^4{K_2}^2+1/20\,\xi^5{K_1}^2+1/20\,\xi^5K_1K_2-\frac{\xi^5A}{60}\\
&+ \left.1/24\,\xi^4A+\frac{\xi^5}{120}-1/24\,\xi^4\right)+1/6\left(\frac{66\,N{K_1}^2R_o}{5}+\frac{72\,NK_1K_2R_o}{5}\right.\\
&+ 6/5\,N{K_2}^2R_o+3/10\,R_oA^2+\frac{22\,{K_1}^2R_o}{35}+\frac{9\,R_oK_1K_2}{35}-\frac{13\,R_o{K_2}^2}{35}\\
&+ \left.2/5\,AR_o-\frac{7\,R_o}{10}\right)\xi^3+1/2\left(-8/5\,N{K_1}^2R_o-6/5\,NK_1K_2R_o\right.\\
&+ 2/5\,N{K_2}^2R_o-1/15\,R_oA^2-\frac{4\,{K_1}^2R_o}{35}-1/35\,R_oK_1K_2+\frac{3\,R_o{K_2}^2}{35}\\
&- \left.1/30\,AR_o+1/10\,R_o\right)\xi^2 \qquad (3.25)
\end{aligned}
$$

$$
\begin{aligned}
h_1(\xi) = -2R_o\Big(&-1/10\,A\xi^5K_1-1/10\,A\xi^5K_2+1/2\,AN\xi^3K_1+1/2\,AN\xi^3K_2\\
&+1/6\,A\xi^4K_1+1/12\,A\xi^4K_2+1/10\,\xi^5K_1+1/10\,\xi^5K_2-AN\xi^2K_1\\
&-1/2\,AN\xi^2K_2-1/2\,K_1\xi^3N-1/2\,\xi^3NK_2-\frac{5\,\xi^4K_1}{12}-1/3\,\xi^4K_2+K_1\xi^2N\\
&+1/2\,\xi^2NK_2+2/3\,K_1\xi^3+1/3\,\xi^3K_2-1/2\,K_1\xi^2\Big)+\Big(-ANK_1R_o\\
&+2/15\,R_oAK_1-1/30\,R_oAK_2+NK_1R_o-3/10\,K_1R_o+1/5\,R_oK_2\Big)\xi \qquad (3.26)
\end{aligned}
$$

$$f_2(\xi) = -\frac{{R_o}^2}{105}\Bigg[\frac{\left(-648\,{K_1}^3 - 1944\,{K_1}^2K_2 - 1944\,K_1{K_2}^2 - 648\,{K_2}^3\right)\xi^{11}}{7920}$$
$$+\frac{\left(3024\,{K_1}^3 + 7560\,{K_1}^2K_2 + 6048\,K_1{K_2}^2 + 1512\,{K_2}^3\right)\xi^{10}}{5040}$$
$$+\frac{\xi^9}{3024}\Bigg(16632\,N{K_1}^3 + 49896\,N{K_1}^2K_2 + 49896\,NK_1{K_2}^2 + 16632\,N{K_2}^3$$
$$+21\,A^2K_1 + 21\,A^2K_2 - 5376\,{K_1}^3 - 10752\,{K_1}^2K_2 - 6216\,K_1{K_2}^2 - 840\,{K_2}^3$$
$$-42\,AK_1 - 42\,AK_2 + 21\,K_1 + 21\,K_2\Bigg) + \frac{\xi^8}{1680}\Bigg(-55440\,N{K_1}^3 - 138600\,N{K_1}^2K_2$$
$$-110880\,NK_1{K_2}^2 - 27720\,N{K_2}^3 + 70\,A^2K_1 + 35\,A^2K_2 + 4200\,{K_1}^3 + 6300\,{K_1}^2K_2$$
$$+2100\,K_1{K_2}^2 + 70\,AK_1 + 140\,AK_2 - 140\,K_1 - 175\,K_2\Bigg) + \frac{\xi^7}{840}\Bigg(-83160\,N^2{K_1}^3$$
$$-249480\,N^2{K_1}^2K_2 - 249480\,N^2K_1{K_2}^2 - 83160\,N^2{K_2}^3 + 210\,A^2NK_1 + 210\,A^2NK_2$$
$$+65184\,N{K_1}^3 + 130872\,N{K_1}^2K_2 + 75432\,NK_1{K_2}^2 + 9744\,N{K_2}^3 - 84\,A^2K_1 + 126\,A^2K_2$$
$$-420\,ANK_1 - 420\,ANK_2 - 996\,{K_1}^3 - 888\,{K_1}^2K_2 - 48\,K_1{K_2}^2 - 156\,{K_2}^3 + 28\,AK_1 - 112\,AK_2$$
$$+210\,NK_1 + 210\,NK_2 + 476\,K_1 + 406\,K_2\Bigg) + \frac{\xi^6}{360}\Bigg(166320\,N^2{K_1}^3 + 415800\,N^2{K_1}^2K_2$$
$$+332640\,N^2K_1{K_2}^2 + 83160\,N^2{K_2}^3 + 840\,A^2NK_1 + 420\,A^2NK_2 - 29232\,N{K_1}^3 - 44604\,N{K_1}^2K_2$$
$$-15372\,NK_1{K_2}^2 - 168\,A^2K_1 - 105\,A^2K_2 + 210\,ANK_1 + 1050\,ANK_2 - 336\,{K_1}^3$$
$$-330\,{K_1}^2K_2 + 138\,K_1{K_2}^2 + 132\,{K_2}^3 + 21\,AK_1 - 105\,AK_2 - 1050\,NK_1 - 1470\,NK_2 - 693\,K_1$$
$$-210\,K_2\Bigg) + \frac{\xi^5}{120}\Bigg(1890\,A^2N^2K_1 + 1890\,A^2N^2K_2 - 101304\,N^2{K_1}^3 - 205632\,N^2{K_1}^2K_2$$
$$-122472\,N^2K_1{K_2}^2 - 18144\,N^2{K_2}^3 - 966\,A^2NK_1 - 756\,A^2NK_2 - 3780\,AN^2K_1 - 3780\,AN^2K_2$$
$$+2448\,N{K_1}^3 + 2052\,N{K_1}^2K_2 + 540\,NK_1{K_2}^2 + 936\,N{K_2}^3 + 119\,A^2K_1 - 14\,A^2K_2$$
$$+252\,ANK_1 - 588\,ANK_2 + 1890\,N^2K_1 + 1890\,N^2K_2 + 132\,{K_1}^3 + 54\,{K_1}^2K_2 - 78\,K_1{K_2}^2$$
$$-98\,AK_1 + 98\,AK_2 + 714\,NK_1 + 1344\,NK_2 + 399\,K_1 - 84\,K_2\Bigg)\Bigg] + \ldots\ldots\ldots \quad (3.27)$$

Table 1: Different cases of stretchability

case	K_1	K_2
1	0	0.5
2	0.5	0.5
3	0.5	0

$$h_2(\xi) = \frac{{R_o}^2}{210}\left[\frac{\xi^9}{72}\left(-204\,A{K_1}^2 - 408\,AK_1K_2 - 204\,A{K_2}^2 + 204\,{K_1}^2 + 408\,K_1K_2 \right.\right.$$
$$\left. + 204\,{K_2}^2\right) + \frac{\xi^8}{56}\left(784\,A{K_1}^2 + 1176\,AK_1K_2 + 392\,A{K_2}^2 - 1036\,{K_1}^2 - 1680\,K_1K_2\right.$$
$$\left. - 644\,{K_2}^2\right) + 1/42\left(2394\,NA{K_1}^2 + 4788\,NAK_1K_2 + 2394\,NA{K_2}^2 - 28\,A^3\right.$$
$$- 1064\,A{K_1}^2 - 1064\,AK_1K_2 - 140\,A{K_2}^2 - 2394\,N{K_1}^2 - 4788\,NK_1K_2 - 2394\,N{K_2}^2$$
$$\left. + 84\,A^2 + 2072\,{K_1}^2 + 2576\,K_1K_2 + 644\,{K_2}^2 - 84\,A + 28\right)\xi^7$$
$$+ 1/30\left(-6300\,NA{K_1}^2 - 9450\,NAK_1K_2 - 3150\,NA{K_2}^2 + 420\,A{K_1}^2 + 210\,AK_1K_2\right.$$
$$+ 8820\,N{K_1}^2 + 14490\,NK_1K_2 + 5670\,N{K_2}^2 - 140\,A^2 - 1960\,{K_1}^2 - 1750\,K_1K_2$$
$$\left. - 280\,{K_2}^2 + 280\,A - 140\right)\xi^6 + 1/20\left(-2520\,N^2A{K_1}^2 - 5040\,N^2AK_1K_2\right.$$
$$- 2520\,N^2A{K_2}^2 + 70\,NA^3 + 5348\,NA{K_1}^2 + 5516\,NAK_1K_2 + 728\,NA{K_2}^2$$
$$+ 2520\,N^2{K_1}^2 + 5040\,N^2K_1K_2 + 2520\,N^2{K_2}^2 + 42\,A^3 - 210\,NA^2 + 200\,A{K_1}^2$$
$$+ 120\,AK_1K_2 - 80\,A{K_2}^2 - 12068\,N{K_1}^2 - 15596\,NK_1K_2 - 4088\,N{K_2}^2 + 14\,A^2$$
$$\left.\left. + 210\,NA + 780\,{K_1}^2 + 440\,K_1K_2 + 220\,{K_2}^2 - 294\,A - 70\,N + 238\right)\xi^5\right] + \ldots\ldots \quad (3.28)$$

The value of $f_3(\xi)$ and $h_3(\xi)$ are too lengthy to be mention. The values of $f(\xi)$ and $h(\xi)$ can be obtained after substituting the values of f_i, h_i $(i = 0, 1, 2, 3)$ in the equations (3.12) and (3.13). In **case 1**, when the upper disk is getting stretched but lower disk is not stretched, $f(\xi)$ and $h(\xi)$ for specific values $K_1 = 0, K_2 = 0.5, R_o = 10, N = 0.1, A = 0.5$ are

$$\begin{aligned} f(\xi) &= -0.00312485\,\xi^{15} + 0.0156243\,\xi^{14} + 0.00690224\,\xi^{13} - 0.119596\,\xi^{12} \\ &+ 0.0588717\,\xi^{11} + 0.225700\,\xi^{10} + 0.183324\,\xi^9 - 0.953439\,\xi^8 + 0.546993\,\xi^7 \\ &+ 0.577577\,\xi^6 - 0.536506\,\xi^5 + 0.0583129\,\xi^4 + 0.0227114\,\xi^3 \\ &- 0.0833504\,\xi^2 \end{aligned} \quad (3.29)$$

$$\begin{aligned} h(\xi) &= -0.0665307\,\xi^{13} + 0.437109\,\xi^{12} - 0.756764\,\xi^{11} - 0.221506\,\xi^{10} \\ &+ 1.08009\,\xi^9 + 0.197704\,\xi^8 - 0.371151\,\xi^7 - 0.333662\,\xi^6 + 1.14274\,\xi^5 \\ &- 2.06742\,\xi^4 + 0.880162\,\xi^3 - 0.243070\,\xi^2 - 0.177707\,\xi + 1 \end{aligned} \quad (3.30)$$

In **case 2**, when both disks are getting stretched, $f(\xi)$ and $h(\xi)$ for specific values $K_1 = 0.5, K_2 = 0.5, R_o = 10, N = 0.1, A = 0.5$ are

$$\begin{aligned} f(\xi) &= -0.0499976\,\xi^{15} + 0.374982\,\xi^{14} - 0.653025\,\xi^{13} - 1.41371\,\xi^{12} + 5.56761\,\xi^{11} \\ &- 3.20133\,\xi^{10} - 7.39027\,\xi^9 + 10.6239\,\xi^8 - 0.379992\,\xi^7 - 8.76374\,\xi^6 \\ &+ 8.87515\,\xi^5 - 5.34507\,\xi^4 + 2.98047\,\xi^3 - 1.72503\,\xi^2 + 0.500000\,\xi \end{aligned} \quad (3.31)$$

$$\begin{aligned} h(\xi) &= -0.532246\,\xi^{13} + 4.53102\,\xi^{12} - 13.6972\,\xi^{11} + 14.7568\,\xi^{10} + 8.46025\,\xi^{9} \\ &- 36.0726\,\xi^{8} + 33.8676\,\xi^{7} - 5.69780\,\xi^{6} - 17.1663\,\xi^{5} + 21.6626\,\xi^{4} - 15.7763\,\xi^{3} \\ &+ 6.39303\,\xi^{2} - 1.22885\,\xi + 1 \end{aligned} \tag{3.32}$$

In **case 3**, when the lower disk is getting stretched but upper disk is not stretched, $f(\xi)$ and $h(\xi)$ for specific values $K_1 = 0.5, K_2 = 0, R_o = 10, N = 0.1, A = 0.5$ are

$$\begin{aligned} f(\xi) &= -0.00312485\,\xi^{15} + 0.0312485\,\xi^{14} - 0.102468\,\xi^{13} + 0.0442971\,\xi^{12} \\ &+ 0.489653\,\xi^{11} - 1.18058\,\xi^{10} + 0.870068\,\xi^{9} + 0.527294\,\xi^{8} - 1.35263\,\xi^{7} \\ &+ 0.713135\,\xi^{6} + 0.630089\,\xi^{5} - 1.42785\,\xi^{4} + 1.50936\,\xi^{3} \\ &- 1.24850\,\xi^{2} + 0.5\,\xi \end{aligned} \tag{3.33}$$

$$\begin{aligned} h(\xi) &= -0.0665307\,\xi^{13} + 0.695647\,\xi^{12} - 2.84370\,\xi^{11} + 5.47795\,\xi^{10} - 3.44647\,\xi^{9} \\ &- 6.27998\,\xi^{8} + 16.2582\,\xi^{7} - 14.8495\,\xi^{6} + 2.71625\,\xi^{5} + 8.49723\,\xi^{4} \\ &- 11.1228\,\xi^{3} + 6.14115\,\xi^{2} - 1.67749\,\xi + 1 \end{aligned} \tag{3.34}$$

In radial directions shear stress at lower disk is denoted by τ_{zr}, which is defined as

$$\tau_{zr} = \mu_1 \left[\frac{\partial u}{\partial z}\right]_{z=0} = \frac{\mu_1 r \omega_1}{\ell} f''(0)$$

4 Results and Discussion

the author presented and analyzed outcomes of the theory in tabular form along with graphs. To fulfill the objective, we choose to present shear stress at the lower disk and flow of velocities for the different parameters. All the considered cases of stretchability are shown in Table 1. These values are taken arbitrarily to analyze the present model as chosen customarily in the literature by [28], [9].

To validate the present result of the study, a comparison between the results achieved by HPM and NM is done. The value of different parameters for comparison are taken as a non-Newtonian parameter $N = 0.1$, Reynolds number $R_o = 10$ and rotation parameter $A = 0.5$. A comparison between HPM and NM is shown graphically in Figure 2 for all three cases of stretchability. The error between the results obtained by HPM and NM is tabulated in Table 2-Table 4 which gives a good agreement. The formula for calculating an error between the results is

$$error = \mid f_{HPM} - f_{NM} \mid$$

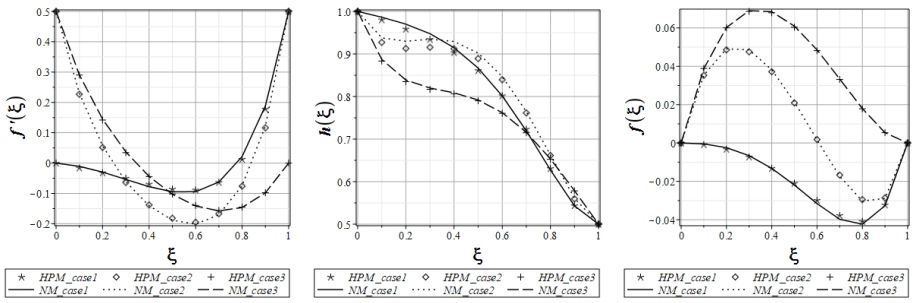

(a) Radial Velocity (b) Transverse Velocity (c) Axial Velocity

Figure 2: Matching results of flow profile of HPM and NM for $N = 0.1$, $R_o = 10$ and $A = 0.5$. Solid lines represent case1, dotted lines represent case2 and dashed lines represent case3

Table 2: Error in values of radial velocity profile calculated by HPM and NM when $K_1 = 0$, $K_2 = 0.5$, $R_o = 10$, $N = 0.1$, $A = 0.5$

ξ	HPM	NM	Error
0.2	-0.0317791250	-0.0299096836	0.0018694414
0.4	-0.0691671858	-0.0777960511	0.0086288652
0.6	-0.0885581670	-0.0943947661	0.0058365991
0.8	0.0127247939	0.0216767469	0.0089519530
1	0.5000000000	0.5000000000	0.0000000000

Table 3: Error in values of transverse velocity profile calculated by HPM and NM when $K_1 = 0$, $K_2 = 0.5$, $R_o = 10$, $N = 0.1$, $A = 0.5$

ξ	HPM	NM	Error
0.2	0.9588096810	0.9700891182	0.0112794372
0.4	0.9035215361	0.9146988296	0.0111772935
0.6	0.8019349578	0.8014292526	0.0005057052
0.8	0.6309745630	0.6274739615	0.0035006015
1	0.5000000000	0.5000000000	0.0000000000

Table 4: Error in values of axial velocity profile calculated by HPM and NM when $K_1 = 0$, $K_2 = 0.5$, $R_o = 10$, $N = 0.1$, $A = 0.5$

ξ	HPM	NM	Error
0.2	-0.0031890742	-0.0024316401	0.0007574341
0.4	-0.0131741919	-0.0132069443	0.0000327524
0.6	-0.0298309610	-0.0315776038	0.0017466428
0.8	-0.0408378869	-0.0423305430	0.0014926561
1	0.0000000000	0.0000000000	0.0000000000

Another source of verification of present results is Table 5-7 in which the results calculated by HPM and NM have been compared with the literature results [28]. Turkyilmazoglu [28] computed the values of shear stress on the lower disk in the radial and tangential directions for all three cases of stretchability, mentioned in Table 1, for $R_o = 0$ and $R_o = 10$. A perfect verification of the results obtained by NM and HPM for the case of Newtonian fluid with the literature can be seen in Table 5-7. This comparison confirms the guarantee of the present attempt.

Table 5: Numeric data of $f''(0)$ for $A = -0.5, 0, 0.5$ when $K_1 = 0$, $K_2 = 0.5$, $N = 0$

Rotation Parameter	$R_o = 0$ [28]	NM (Present)	HPM (Present)	$R_o = 10$ [28]	NM (Present)	HPM (Present)
A = -0.5	-1.00000000	-1.00000000	-1.00000000	0.19385791	0.19385790	0.20503384
A = 0	-1.00000000	-1.00000000	-1.00000000	0.047184	0.04718399	0.05987216
A = 0.5	-1.00000000	-1.00000000	-1.00000000	-0.36279802	-0.36279801	-0.35464816

Table 6: Numeric data of $f''(0)$ for $A = -0.5, 0, 0.5$ when $K_1 = 0.5$, $K_2 = 0.5$, $N = 0$

Rotation Parameter	$R_o = 0$ [28]	NM (Present)	HPM (Present)	$R_o = 10$ [28]	NM (Present)	HPM (Present)
A = -0.5	-3.00000009	-3.00000000	-3.00000000	-2.26713850	-2.26713850	-2.26383874
A = 0	-3.00000009	-2.99999999	-3.00000000	-2.38938053	-2.38938053	-2.38462036
A = 0.5	-3.00000009	-3.00000000	-3.00000000	-3.00199603	-3.00199604	-3.02297732

Table 7: Numeric data of $f''(0)$ for $A = -0.5, 0, 0.5$ when $K_1 = 0.5$, $K_2 = 0$, $N = 0$

Rotation Parameter	$R_o = 0$ [28]	NM (Present)	HPM (Present)	$R_o = 10$ [28]	NM (Present)	HPM (Present)
A = -0.5	-2.00000007	-2.00000000	-2.00000000	-1.60562889	-1.60562889	-1.59405521
A = 0	-2.00000007	-2.00000000	-2.00000000	-1.44561724	-1.44561724	-1.44174574
A = 0.5	-2.00000007	-2.00000000	-2.00000000	-1.89459839	-1.89459839	-1.89315515

The nature of $f'(\xi)$, $h(\xi)$ and $f(\xi)$ for the different values of R_o, non-Newtonian parameter N and rotation parameter A are presented graphically in Figure 3 - 11. Also, the behavior of velocities are discussed in three different cases of stretchability when (1) the upper disk is getting stretched but the lower disk is not stretched (2) both disks are getting stretched (3) the lower disk is getting stretched but the upper disk is not stretched.

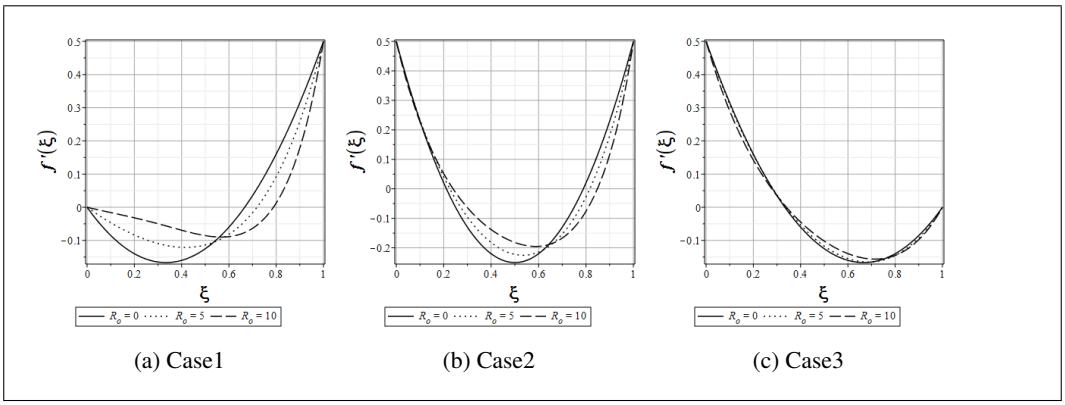

(a) Case1 (b) Case2 (c) Case3

Figure 3: Radial velocity for different R_o when $N = 0.1$, $A = 0.5$

The performance of velocity profile for distinct values of R_o when $N = 0.1$ and $A = 0.5$ is presented in Figure 3a-3c. Figure 3 displays the variation of radial velocity for all three cases of stretchability. Figure 3a analyzes that the radial velocity falls in the nearby area of the lower boundary while raise in the nearby area of the upper boundary. Also, near the lower disk, velocity rises with the rise in R_o but its nature is opposite near the upper disk. Figure 3b reflects symmetric nature of radial velocity in case2. This figure displays that the minimum value of radial velocity shifts towards the upper disk as increasing the Reynolds number. Also, it decreases with an increase of R_o near the upper disk. Figure 3c analyzes the behavior of the velocity in case3. This figure tells that velocity decreases from the stretching parameter of the lower disk very rapidly but increases near the upper disk. The magnitude of radial velocity decreases for increasing values of R_o near the upper disk in all the cases of stretchability. It is because of that as we increase the value of R_o, the inertial force increases which reduces the fluid motion.

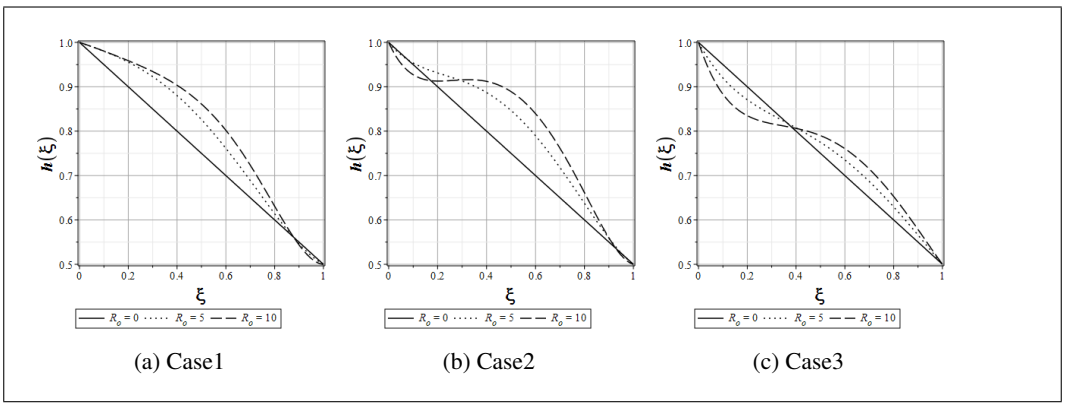

(a) Case1 (b) Case2 (c) Case3

Figure 4: Transverse velocity for different R_o when $N = 0.1$, $A = 0.5$

The behavior of transverse velocity for different cases of stretchability is presented in Figure 4a-4c. It is clear from all three cases that when $R_o = 0$, velocity declines linearly from the lower end to the upper end. In Figure 4a, velocity rises with a rise in the values of R_o while it falls down in the nearby of the upper disk with an increase in R_o due to stretching and rotation in the upper disk. The opposite behavior can be seen in Figure 4c.

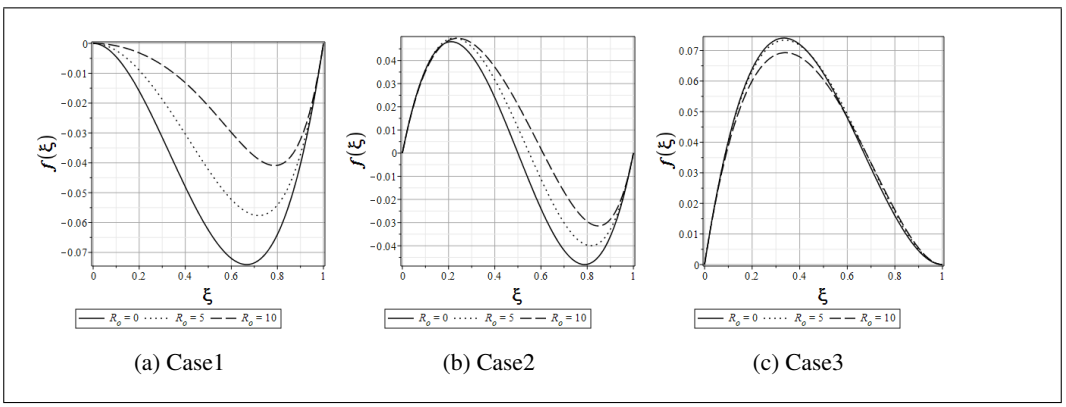

(a) Case1 (b) Case2 (c) Case3

Figure 5: Axial velocity for different R_o when $N = 0.1$, $A = 0.5$

The variation of axial velocity for three cases of stretchability is presented in Figure 5a-5c. Figure 5a says that the $f(\xi)$ increases with an increase in R_o. In Figure 5b, the fluid is moving outwards over the faster-rotating disk and moving inside over the slower rotating disk. This figure also shows the same behavior but no change can be seen near the lower and upper disks. Figure 5c analyzes that velocity achieves its maximum value near the lower disk. A decrement in the velocity with an increment in R_o near the lower disk can be observed while its nature is opposite near the upper disk.

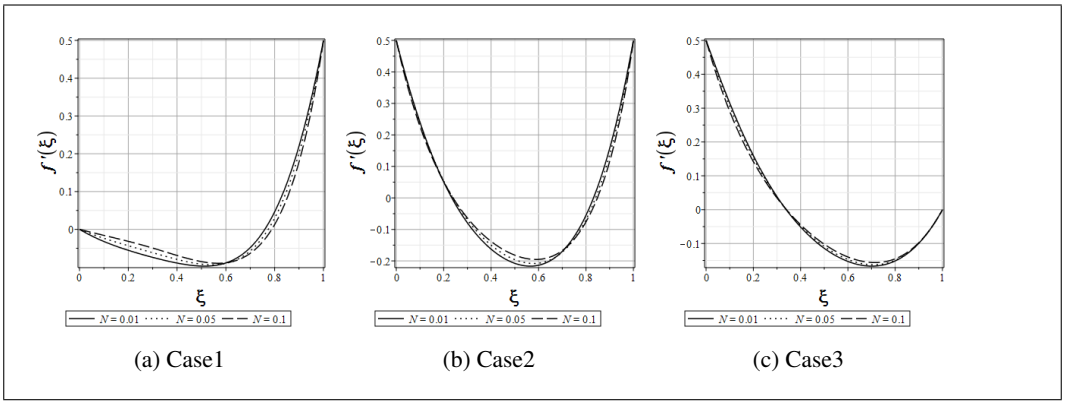

(a) Case1 (b) Case2 (c) Case3

Figure 6: Radial velocity for different N when $R_o = 10$, $A = 0.5$

The effect of non-Newtonian parameter $N = 0.01, 0.05, 0.1$, in all three cases of stretchability, when $R_o = 10$ and $A = 0.5$ on the $f^{'}(\xi)$ is presented in Figure 6. Figure 6a depicts that velocity decreases near the lower disk but increases rapidly near the upper disk. Also, on increasing the value of N, velocity is increasing near the lower disk while its behavior is reversed near the upper disk. Figure 6b investigates the symmetric behavior of velocity. Figure 6c analyzes that the velocity decreases sharply from the stretching parameter of the lower disk while it increases near the upper disk.

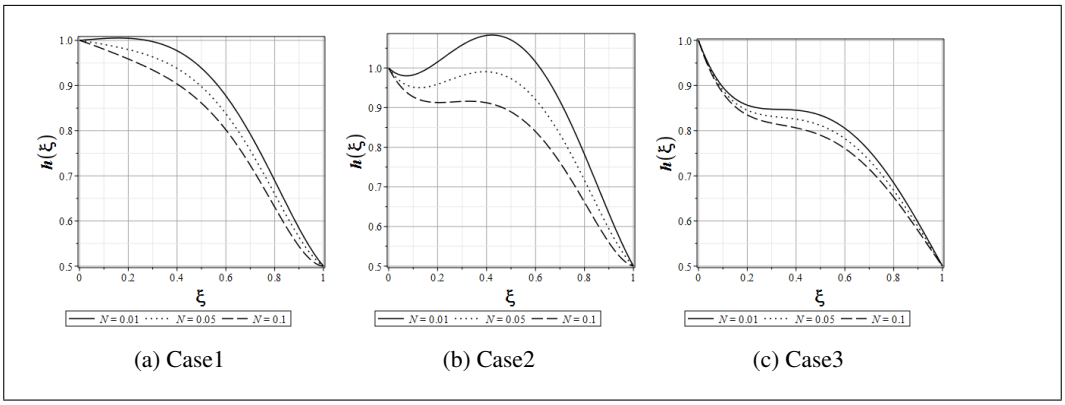

(a) Case1 (b) Case2 (c) Case3

Figure 7: Transverse velocity for different N when $R_o = 10$, $A = 0.5$

The variation of $h(\xi)$ for different N is presented in Figure 7. Figure 7a-7c present case1, case2 and case3 respectively. Figure 7a analyzes that velocity increases slightly near the lower disk and then decreases up to the upper disk. Figure 7b analyzes the behavior of transverse velocity when both the disks are getting stretched. In Figure 7c, velocity decreases from the lower end to the upper end.

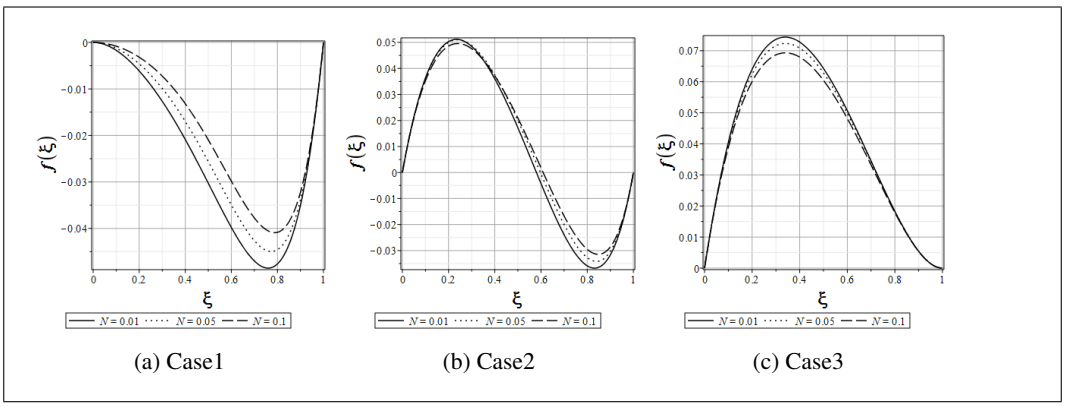

(a) Case1 (b) Case2 (c) Case3

Figure 8: Axial velocity for different N when $R_o = 10$, $A = 0.5$

The variation of axial velocity for different value of non-Newtonian parameter N when $R_o = 10$ and $A = 0.5$ is discussed in Figure 8. The behavior of $f(\xi)$ in case1 is shown in figure 8a. When the lower disk is getting stretched and the upper disk is not stretching, axial velocity decreases rapidly from the lower disk whereas it increases fastly near the upper disk. It is also clear that velocity increases with an increase in N while its magnitude is almost the same near the upper disk. Figure 8b presents axial velocity behavior when both disks are getting stretched. It can be seen from this figure that axial velocity is positive near the lower disk but negative near the upper disk. It can also be observed that velocity gets its maximum value near the lower disk while gets its minimum value near the upper disk. Also, velocity decreases with an increase in N near the lower disk while its behavior is reversed near the upper disk. Figure 8c shows the behavior of axial velocity in case3. It is clear from this figure that velocity achieves its maximum value near the lower disk. Also, velocity decreases with an increase of N while near both disks, there is no specific change in velocity.

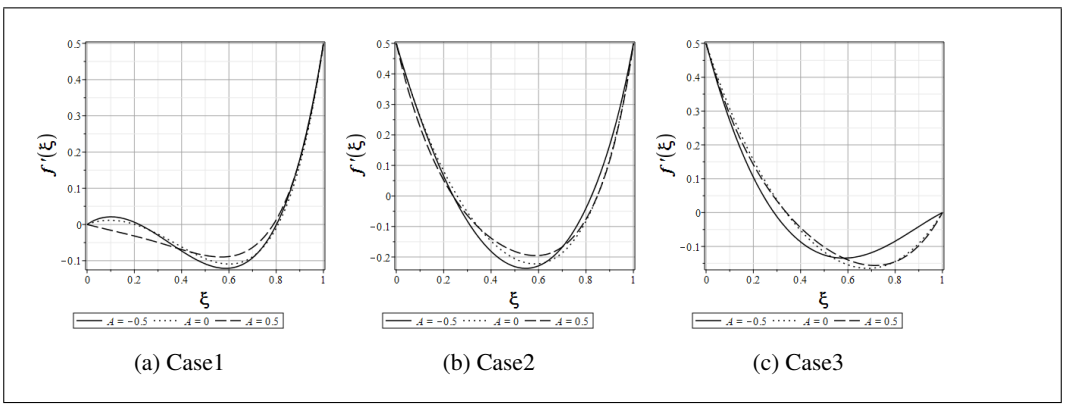

(a) Case1 (b) Case2 (c) Case3

Figure 9: Radial velocity for different A when $R_o = 10$, $N = 0.1$

Figure 9 explains the behavior of radial velocity for all cases of stretchability. In this section, $A < 0$ means lower and upper disks are rotating in opposite directions, $A = 0$ means there is no rotation in the upper disk, and $A > 0$ means both disks are rotating in the same directions. Figure 9a is discussed for case1 of stretchability. This figure depicts that when $A = -0.5, 0$, there is a small increment in the magnitude of the radial velocity near the lower disk while near the upper disk it increases rapidly. when $A = 0.5$, velocity decreases up to $\xi \sim 0.6$ then increases up to the stretching parameter of the upper disk. It can also be observed that velocity increases with an increase in A near the region $0.4 < \xi < 0.7$. Figure 9b is discussed when both disks are getting stretched. This figure analyses that the behavior of the velocity is symmetric. Also, the minimum value of velocity shifts towards the upper disk on increasing the value of the rotation parameter A. It can also be seen that radial velocity increases with an increase in A near the middle region

of disks. In figure 9c, case3 is discussed. According to this figure, velocity decreases rapidly from the lower disk but increases near the upper disk.

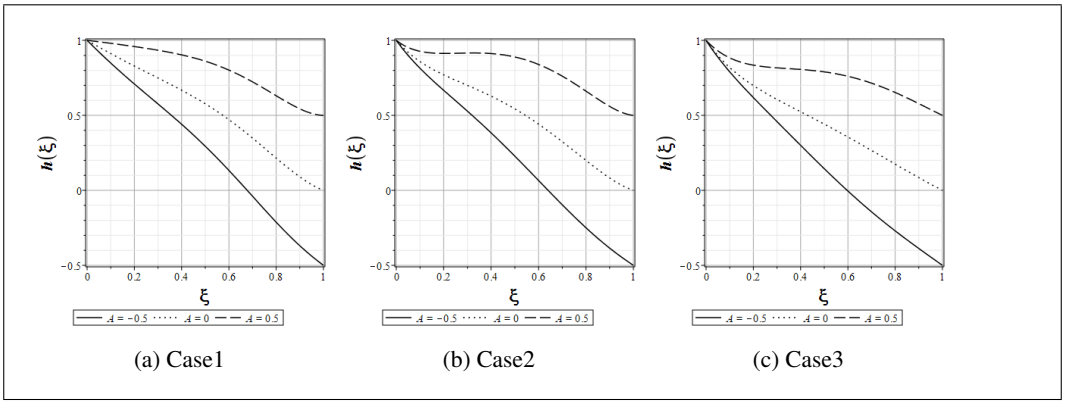

(a) Case1 (b) Case2 (c) Case3

Figure 10: Transverse velocity for different A when $R_o = 10$, $N = 0.1$

Figure 10 explains the behavior of transverse velocity for all cases of stretchability. This figure depicts that when lower and upper disks are rotating in opposite directions i.e.$A < 0$, and when there is no rotation in the upper disk i.e.$A = 0$, the behavior of transverse velocity is almost the same in all cases of stretchability. It is also clear from Figure 10a-10c that velocity decreases from lower disk to the stretching parameter of upper disk (K_2). It can also be noted from Figure 10 that velocity increases with an increase in rotation parameter.

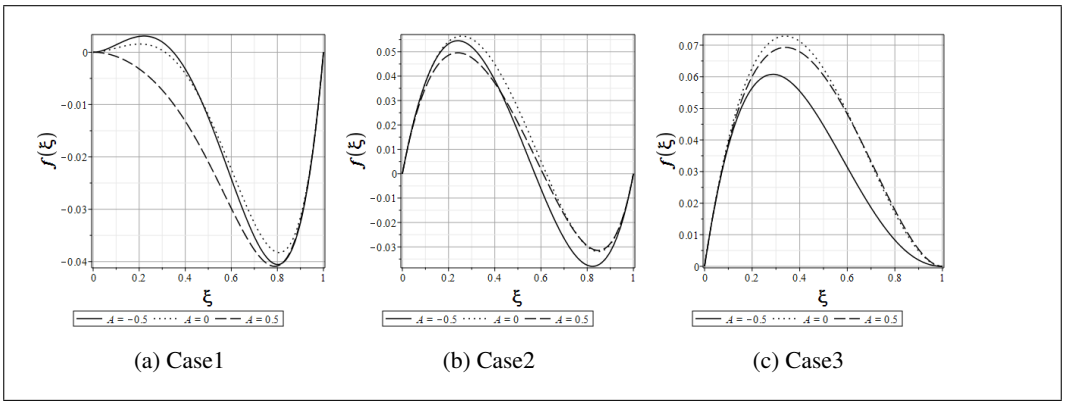

(a) Case1 (b) Case2 (c) Case3

Figure 11: Axial velocity for different A when $R_o = 10$, $N = 0.1$

Figure 11 explains the behavior of axial velocity for all cases of stretchability. Figure 11a depicts that when $A = -0.5, 0$, axial velocity decreases in the region $0.2 < \xi < 0.8$ after a small increment in magnitude in the region $0 < \xi < 0.2$ and increases rapidly near the upper disk. when $A = 0.5$, axial velocity decreases up to the region $\xi \sim 0.8$ and increases sharply up to the upper disk. Figure 11b shows that the behavior of axial velocity is symmetric but opposite along $z = 0$. It can also be observed that when both disks are getting radially stretched, velocity gets its maximum value near the lower disk while gets its minimum value near the upper disk. Figure 11c shows that axial velocity is positive throughout the gap length. Its behavior is almost the same for a different value of A. This figure also investigates that velocity increases rapidly near the stretching disk and decreases up to the non-stretching disk. It can also be noted that when there is no rotation, velocity achieves its maximum value.

5 Conclusion

In this article, a flow of Reiner-Rivlin fluid between two rotating stretchable disks is studied. The Homotopy Perturbation Method is successfully employed in this model. This study is done for three cases of stretchability, when the upper disk is getting stretched but the lower disk is not stretched, when both disks are getting stretched, and when the lower disk is getting stretched but the upper disk is not stretched. The effect of Reynolds number R_o, the non-Newtonian parameter N, and rotation parameter A on velocity profiles are discussed and shown graphically. The following key points can be concluded

- The comparison between HPM and NM shows that the proposed analytical method is highly accurate and provides rapid achievement to compute the flow velocities.
- By substituting the non-Newtonian parameter $N = 0$, the results are verified by [28].
- Shear stress on the lower disk in the radial direction for all three cases of stretchability is compared with literature [28], which also verified the accuracy of results.
- When both disks are stretching, the behavior of radial velocity is the same for all parameters.
- Minimum value of radial velocity shifts towards the upper disk in case2 of stretchability.
- Transverse velocity decreases from the lower disk to the upper disk for different values of Reynolds number and non-Newtonian parameter.
- The behavior of axial velocity is the same for different values of R_o and N.

References

[1] Reshu Agarwal. Analytical study of micropolar fluid flow between two porous disks. *PalArch's Journal of Archaeology of Egypt/Egyptology*, 17(12):903–924, 2020.

[2] Reshu Agarwal. Heat and mass transfer in electrically conducting micropolar fluid flow between two stretchable disks. *Materials Today: Proceedings*, 2021.

[3] Reshu Agarwal and Pankaj Kumar Mishra. Analytical solution of the mhd forced flow and heat transfer of a non-newtonian visco-inelastic fluid between two infinite rotating disks. *Materials Today: Proceedings*, 2021.

[4] P Donald Ariel. The homotopy perturbation method and analytical solution of the problem of flow past a rotating disk. *Computers & Mathematics with Applications*, 58(11-12):2504–2513, 2009.

[5] Go K Batchelor. Note on a class of solutions of the navier-stokes equations representing steady rotationally-symmetric flow. *The quarterly journal of mechanics and applied mathematics*, 4(1):29–41, 1951.

[6] WG Cochran. The flow due to a rotating disc. In *Mathematical Proceedings of the Cambridge Philosophical Society*, volume 30, pages 365–375, 1934.

[7] Bernard D Coleman and Walter Noll. An approximation theorem for functionals, with applications in continuum mechanics. In *The foundations of mechanics and thermodynamics*, pages 97–112. 1974.

[8] Abhijit Das and Bikash Sahoo. Flow of a reiner-rivlin fluid between two infinite coaxial rotating disks. *Mathematical Methods in the Applied Sciences*, 41(14):5602–5618, 2018.

[9] Abhijit Das and Suman Sarkar. Flow analysis of reiner–rivlin fluid between two stretchable rotating disks. In *Recent Trends in Wave Mechanics and Vibrations*, pages 61–70. 2020.

[10] Saeed Dinarvand. On explicit, purely analytic solutions of off-centered stagnation flow towards a rotating disc by means of ham. *Nonlinear Analysis: Real World Applications*, 11(5):3389–3398, 2010.

[11] Deog-Hee Doh, M Muthtamilselvan, B Swathene, and E Ramya. Homogeneous and heterogeneous reactions in a nanofluid flow due to a rotating disk of variable thickness using ham. *Mathematics and Computers in Simulation*, 168:90–110, 2020.

[12] Tasawar Hayat, Mehwish Javed, Maria Imtiaz, and Ahmed Alsaedi. Convective flow of jeffrey nanofluid due to two stretchable rotating disks. *Journal of Molecular Liquids*, 240:291–302, 2017.

[13] Ji-Huan He. Homotopy perturbation technique. *Computer methods in applied mechanics and engineering*, 178(3-4):257–262, 1999.

[14] Ji-Huan He. A coupling method of a homotopy technique and a perturbation technique for non-linear problems. *International journal of non-linear mechanics*, 35(1):37–43, 2000.

[15] Ji-Huan He et al. Recent development of the homotopy perturbation method. *Topological methods in nonlinear analysis*, 31(2):205–209, 2008.

[16] GN Lance and MH Rogers. The axially symmetric flow of a viscous fluid between two infinite rotating disks. *Proceedings of the Royal Society of London. Series A. Mathematical and Physical Sciences*, 266(1324):109–121, 1962.

[17] M Maeder, R D'Auria, E Grasso, G Petrone, S De Rosa, M Klaerner, L Kroll, and S Marburg. Numerical analysis of sound radiation from rotating discs. *Journal of Sound and Vibration*, 468:115085, 2020.

[18] Syed Muhammad Raza Shah Naqvi, Hyun Min Kim, Taseer Muhammad, Fouad Mallawi, and Malik Zaka Ullah. Numerical study for slip flow of reiner-rivlin nanofluid due to a rotating disk, 2020.

[19] PG Jansi Rani, M Kirthiga, Angela Molina, E Laborda, and L Rajendran. Analytical solution of the convection-diffusion equation for uniformly accessible rotating disk electrodes via the homotopy perturbation method. *Journal of Electroanalytical Chemistry*, 799:175–180, 2017.

[20] MM Rashidi, SA Mohimanian Pour, T Hayat, and S Obaidat. Analytic approximate solutions for steady flow over a rotating disk in porous medium with heat transfer by homotopy analysis method. *Computers & Fluids*, 54:1–9, 2012.

[21] Bikash Sahoo and Igor V Shevchuk. Heat transfer due to revolving flow of reiner-rivlin fluid over a stretchable surface. *Thermal Science and Engineering Progress*, 10:327–336, 2019.

[22] Bikash Sahoo, Robert A Van Gorder, and HI Andersson. Steady revolving flow and heat transfer of a non-newtonian reiner–rivlin fluid. *International communications in heat and mass transfer*, 39(3):336–342, 2012.

[23] KR Singh and R Agarwal. Heat transfer in the forced flow of visco-inelastic fluid between two infinite discs. *ACTA CIENCIA INDICA MATHEMATICS*, 32(2):589, 2006.

[24] K Stewartson et al. On the flow between two rotating coaxial disks. In *Proc. Camb. Phil. Soc*, volume 49, pages 333–341, 1953.

[25] Maria Tabassum and M Mustafa. A numerical treatment for partial slip flow and heat transfer of non-newtonian reiner-rivlin fluid due to rotating disk. *International Journal of Heat and Mass Transfer*, 123:979–987, 2018.

[26] M Turkyilmazoglu. Analytic approximate solutions of rotating disk boundary layer flow subject to a uniform suction or injection. *International Journal of Mechanical Sciences*, 52(12):1735–1744, 2010.

[27] M Turkyilmazoglu. Purely analytic solutions of magnetohydrodynamic swirling boundary layer flow over a porous rotating disk. *Computers & Fluids*, 39(5):793–799, 2010.

[28] Mustafa Turkyilmazoglu. Flow and heat simultaneously induced by two stretchable rotating disks. *Physics of Fluids*, 28(4):043601, 2016.

[29] Muhammad Usman, Ahmer Mehmood, and Bernhard Weigand. Heat transfer from a non-isothermal rotating rough disk subjected to forced flow. *International Communications in Heat and Mass Transfer*, 110:104395, 2020.

[30] Th Von Karman. On laminar and turbulent friction. 1946.

[31] Si Xinhui, Zheng Liancun, Zhang Xinxin, and Si Xinyi. Homotopy analysis method for the asymmetric laminar flow and heat transfer of viscous fluid between contracting rotating disks. *Applied Mathematical Modelling*, 36(4):1806–1820, 2012.

[32] Baoheng Yao and Lian Lian. A new analysis of the rotationally symmetric flow in the presence of an infinite rotating disk. *International Journal of Mechanical Sciences*, 136:106–111, 2018.

[33] Baoheng Yao and Lian Lian. Series solution of the rotationally symmetric flow in the presence of an infinite rotating disk with uniform suction. *European Journal of Mechanics-B/Fluids*, 74:159–166, 2019.

[34] MR Zangooee, Kh Hosseinzadeh, and DD Ganji. Hydrothermal analysis of mhd nanofluid (tio2-go) flow between two radiative stretchable rotating disks using agm. *Case Studies in Thermal Engineering*, 14:100460, 2019.

Author information

Reshu Agarwal, Department of Mathematics, University of Petroleum and Energy Studies, Dehradun, India.
E-mail: rgupta@ddn.upes.ac.in